Synthesis of Modular "Inorganic–Organic–Inorganic" Polyoxometalates and Their Assembly into Vesicles**

Chullikkattil P. Pradeep, Mauricio F. Misdrahi, Feng-Yan Li, Jie Zhang, Lin Xu,* De-Liang Long, Tianbo Liu,* and Leroy Cronin*

Polyoxometalates (POMs) are metal oxide cluster compounds with applications in many fields from medicine to nanotechnology.[1] The applicability of POMs can be broadened by attaching organic groups to the cluster, thereby exploiting the synergistic combination of the metal oxide and the organic functionality.[2] Many POM hybrids have been obtained by replacement of terminal oxo ligands with nitrido, hydrazido, and imido ligands, including dimeric species.[2,3] Other examples involve organosilyl,[4] organophosphoryl,[5] and organotin[6] derivatives of lacunary POM clusters. In terms of grafting ligands onto POMs, tris(hydroxymethyl)-aminomethane (Tris) is geometrically well-suited,[7,8] and Tris-grafted POM clusters have opened up new avenues in materials chemistry. For example, Tris-derived Mn-Anderson clusters have been shown to exhibit gel formation and selective cell-adhesion properties.[8] Compared to the smaller and less redox-active Lindqvist and Anderson-type clusters, there is a need to target clusters that are large and more redox-active for the application of hybrids in materials design[9] and catalysis, especially if electronic communication between the moieties is possible.[10]

Also, the construction of POM hybrids that self-assemble into very large structures is an important goal since POMs have the potential to bridge the molecular and macromolecular length scales.[1] This is because self-assembled structures such as vesicles are receiving considerable attention because of their potential as novel compartments, artificial cell membranes, and nanoreactors, as well as drug and gene delivery agents.[11] Furthermore, the design of artificial capsules with functional amphiphiles is challenging.[12–14] In this respect, we have been targeting the synthesis of modular functional POM-based organic–inorganic amphiphiles for vesicle assembly.[15]

Herein we report the synthesis and structural characterization of two members of a new class of "inorganic–organic–inorganic" hybrid molecules derived by grafting linear bis-(Tris) ligands onto the V_3-capped Wells–Dawson-type cluster $TBA_5H_4[P_2V_3W_{15}O_{62}]$, ($TBA = nBu_4N^+$). These hybrids, which are approximately 3.4 nm long, represent the first examples of inorganic–organic–inorganic "dumbbell" hybrids based on the functional Wells–Dawson-type clusters.[3] Furthermore, we show that one of these hybrids self-assembles into vesicles in acetone/water solutions which have been characterized by light scattering and transmission electron microscopy (TEM) techniques.

The linear bis(Tris) linker ligands used in this study, L^1 and L^2, are depicted in Scheme 1. The Wells–Dawson-based
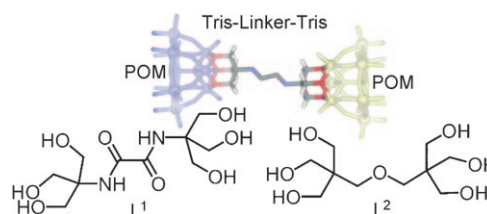
Scheme 1. The modular approach (top) to the hybrids with ligands L^1 and L^2 (bottom).

clusters $TBA_{10}H_2[\{P_2V_3W_{15}O_{59}(OCH_2)_3CNHCO\}_2]$ (**1**) and $TBA_{10}H_2[\{P_2V_3W_{15}O_{59}(OCH_2)_3CCH_2\}_2O]$ (**2**) were synthesized in good yields by heating $TBA_5H_4[P_2V_3W_{15}O_{62}]$ with L^1 and L^2, respectively, at reflux in dry acetonitrile. The compounds thus obtained were characterized by elemental analyses, IR and NMR spectroscopy, ESI-MS, and (in the case of **1**) also by single-crystal X-ray crystallography (Figure 1).[16] As expected, the analytical studies revealed that these hybrids contain two V_3-capped Wells–Dawson-type clusters linked together by the bis(Tris) ligands. Initial investigations into their thermal stability revealed that these compounds are stable up to approximately 225 °C (see the Supporting Information, Figure S1 and S2).

Crystallization of **1** was carried out by diffusion of diethyl ether into an acetonitrile solution of **1** and yellow block crystals were collected after one week. Single-crystal X-ray analysis[16] confirmed that compound **1** contains two

[*] Prof. L. Xu
Key Laboratory of Polyoxometalate Science of Ministry of Education
Department of Chemistry, Northeast Normal University
Changchun, Jilin (P.R. China)
E-mail: linxu@nenu.edu.cn

M. F. Misdrahi,[+] Dr. J. Zhang, Prof. T. Liu
Department of Chemistry, Lehigh University
Bethlehem, PA 18015 (USA)
Fax: (+1) 610-758-6536
E-mail: liu@lehigh.edu
Homepage: http://www.lehigh.edu/~inliu

Dr. C. P. Pradeep,[+] F.-Y. Li,[+] Dr. D.-L. Long, Prof. L. Cronin
WestCHEM, Department of Chemistry, The University of Glasgow
University Avenue, Glasgow G12 8QQ, Scotland (UK)
Fax: (+44) 141-330-4888
E-mail: l.cronin@chem.gla.ac.uk
Homepage: http://www.croninlab.com

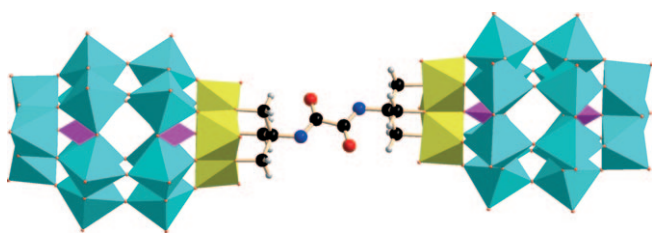[+] These authors contributed equally to this work.

Figure 1. Combined ball-and-stick and polyhedral representation of the molecular structure of the cluster anion in **1**. P pink, W turquoise, N blue, O red, V yellow, C black, H gray.

$\{P_2V_3W_{15}O_{62}\}$ clusters, which are linked together by the bis(Tris) ligand L^1 (Figure 1). In the two $\{P_2V_3W_{15}O_{62}\}$ clusters present in **1**, three oxygen atoms from organic alkoxide groups replace the three bridging oxygen atoms in the V_3 cap of each cluster. The whole unit cell contains 4 cluster-dimer anions and 40 TBA cations which are mostly concentrated around the two cluster heads of the cluster dimers and undergo extensive and exclusive C-H···O hydrogen bonded interactions with the cluster oxygen atoms. Specifically, each TBA cation undergoes 3–6 C-H···O H-bonding interactions with a particular $\{P_2V_3W_{15}O_{62}\}$ cluster and involves in similar H-bonding interactions with another cluster on the neighboring molecules. Thus, the TBA cations are sandwiched between the cluster heads of the adjacent cluster dimers through hydrogen bonds so that the cations effectively wrap around the cluster heads, which are therefore bulkier than their relatively thin middle part (Figure 2). This, together with an unusual zig-zag packing mode of the dimers in the crystal
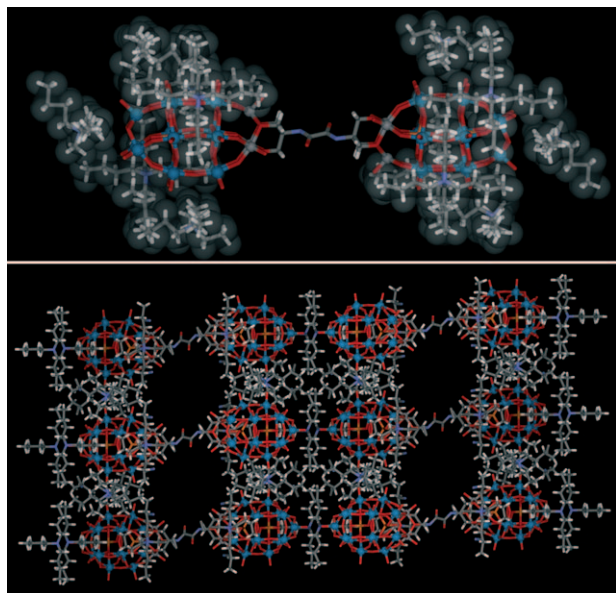

Figure 2. Packing diagram of compound **1** showing the selective gathering of TBA cations around cluster heads leading to voids in the crystal lattice. C gray, H white, N blue, W blue spheres, V gray spheres. The top view shows how the cluster-anion parts of the dimers are encapsulated by the TBA cation (TBA cations shown in stick and space-filling mode). Bottom: View showing the voids and the aggregation of TBA around the clusters.

lattice leads to the formation of 1D channels along the crystallographic *b* axis (see the Supporting Information, Figure S3 and S4). The diameter of these channels is approximately 1 nm and they are filled with disordered CH_3CN solvent molecules. The solvent-accessible void in the channels is approximately 4761 $Å^3$, 15% of the total unit-cell volume.

Therefore it appears that the void space in the crystal lattice is formed because of the selective aggregation of TBA cations around the cluster heads, rather than the organic linker units. The length of the organic linker unit is approximately 1 nm which also coincides with the diameter of the voids (ca. 1 nm). Hence, the crystal structure of **1** suggests that it could be possible to increase the void space in similar dimer systems simply by changing the length of the organic linker units.

In this study, we have also utilized ESI-MS to confirm the composition of compounds **1** and **2**.[17] ESI-MS data of compound **1** in acetonitrile are shown in the Supporting Information (Figure S5 and Table S1). The peaks centered at m/z 2516.7 and 2456.1 correspond to $TBA_8[\{P_2V_3W_{15}O_{59}(OCH_2)_3CNHCO\}_2]^{4-}$ and $TBA_7H[\{P_2V_3W_{15}O_{59}(OCH_2)_3CNHCO\}_2]^{4-}$, respectively. All the major peaks in the ESI-MS spectrum of compound **1** can be assigned to the cluster anion $[\{P_2V_3W_{15}O_{59}(OCH_2)_3CNHCO\}_2]^{12-}$, which is in accordance with the results of elemental analyses and crystallography. Although efforts to grow crystals of **2** were not successful, probably because of the flexibility of the linker L^2, the composition of compound **2** is unambiguously revealed by ESI-MS studies. Similar to the spectrum of **1**, the groups of peaks corresponding to different negative charges (4^-, 5^-, 6^-, etc.) are observed in the ESI-MS spectra of **2** as well; each peak of these groups could be satisfactorily assigned to the formula $[\{P_2V_3W_{15}O_{59}(OCH_2)_3CCH_2\}_2O]^{12-}$ with a varying number of TBA and other counterions. For example, peaks observed at m/z values 3275.5 and 2451.1 correspond to $TBA_7Na_2[\{P_2V_3W_{15}O_{59}(OCH_2)_3CCH_2\}_2O]^{3-}$, $TBA_7Na[\{P_2V_3W_{15}O_{59}(OCH_2)_3CCH_2\}_2O]^{4-}$, respectively (see the Supporting Information, Figure S6 and Table S2).

Inspired by the structure of **1**, which showed a cluster–TBA bilayer-type structure in the solid state, we investigated the possibility that compounds **1/2** could be amphiphilic. Remarkably, both compounds are indeed amphiphilic, acting like surfactants in solution. The study on compound **2**, which is soluble at 0.1 mg mL^{-1} in water/acetone solvents containing less than 60 vol% acetone, is described in detail. The clear solutions of **2** were monitored by using the static light scattering (SLS) and dynamic light scattering (DLS) techniques. Significant scattered intensities were recorded from SLS studies in solutions containing 30–60 vol% acetone, indicating the formation of supramolecular structures (the discrete clusters of **2** can only generate very weak scattered intensity in solution). At the same time, the CONTIN[18a] analysis of the DLS studies provides the average hydrodynamic radius ($R_{h,0}$) of the large structures in solution; as the vesicles show no angular dependence, R_h can be proposed as $R_{h,0}$ (see the Supporting Information; Figure S7 and S8). The relation of $R_{h,0} \approx R_g$ for the large assemblies is observed in all the solutions, suggesting a hollow spherical vesicular structure.[18b]

This is confirmed by TEM studies on these large assemblies, as shown in Figure 3, where a remarkable contrast between the central areas and the black periphery of **2** is observed.
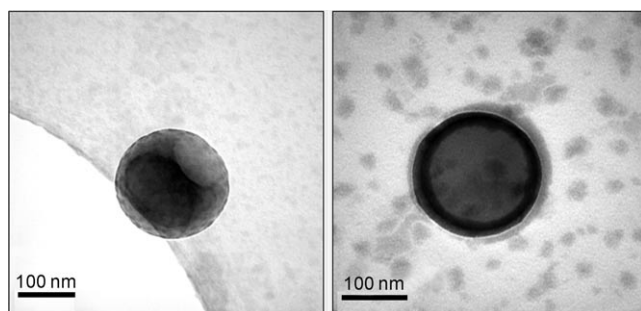

Figure 3. TEM images showing a hollow vesicle structure of the self-assembly of compound **2** in solution.

The vesicle size increases with increasing acetone content in the solvent, ranging from around 61 to 83 nm in solutions containing 30–60 vol% acetone, respectively, for 0.10 mg mL^{-1} solutions of **2**. Figure 4a shows that a linear
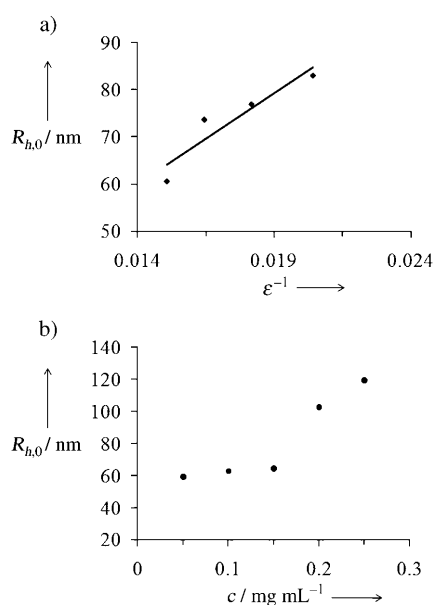

Figure 4. a) Hydrodynamic radius ($R_{h,0}$) as a function of the inverse dielectric constant of acetone/water; b) $R_{h,0}$ as a function of the concentration of compound **2**.

relationship is found between the $R_{h,0}$ of the vesicles and the inverse of the dielectric constant. This is the typical feature for a charge-regulated self-assembly process.[19,20] In a fixed solvent (50:50 vol% water/acetone), the vesicle size of **2** shows a concentration dependence in the range of 0.05–0.25 mg mL^{-1}. DLS studies indicate that the average vesicle size remains constant around 60 nm when concentration of **2** is ≤ 0.15 mg mL^{-1}. At higher concentrations, the $R_{h,0}$ value

increases with increasing concentration to up to 120 nm (Figure 4b).

Vesicle structures are common in surfactant systems. However, the formation of vesicles by the current inorganic–organic–inorganic hybrids is unique due to their very large polar head groups. Vesicle formation requires the closed packing of the solvophobic part into a bilayer membrane structure.[21] In the presence of large POM head group, the closed packing of the organic linker becomes very difficult because the number of linkers in the solvophobic region is limited. For conventional surfactants, such a case usually leads to the formation of spherical micelles in which the solvent-phobic part is less dominant. However, our studies clearly indicate that the vesicles are the assembled structures. A possible explanation is that the countercations of the dimer hybrids, TBA, play an important role.[22] Each TBA cation possesses four n-C$_4$H$_9$ chains whose length is close to that of the hydrophobic linker of the dumbbell. For each anionic dimer-cluster hybrid, if some of its 10 TBA cations can take part in the self-assembly by placing their alkyl chains into the solvophobic region, the region can be successfully filled with hydrophobic components and thus satisfy the requirements for the vesicle formation. Furthermore, the placement of some counterions on the vesicle surface between POM polar head groups can effectively decrease the electrostatic repulsion among the highly charged dumbbell clusters and thus further stabilize the assembled structures. Based on this, a model is presented in Figure 5 to demonstrate the possible
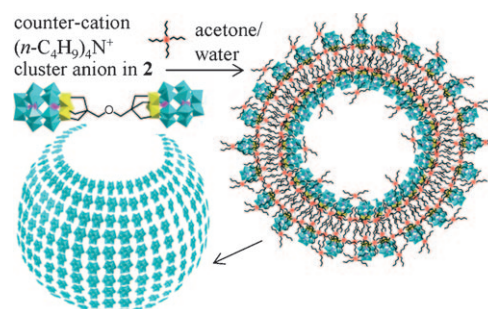

Figure 5. Dimeric anion **2** and TBA countercations forming a vesicle in acetone/water solutions.

vesicle structure formed by such novel materials. The vesicles are still negatively charged overall, but most of the remaining counterions are closely associated to the external and internal surfaces of the vesicles, as confirmed by the Zeta potential studies.[23] Comparison of the proposed solution structure of **2** with the crystal structure of **1** therefore points to occurrence of rearrangements and reorientations of TBA cations during the self-assembly of such cluster dimers in solution, facilitating the suprastructure formation. It would be interesting to examine the effect of countercations on the vesicle formation in further work.

In summary, we have designed and developed a new class of nanometer-sized (ca. 3.4 nm) hybrids starting from Wells–Dawson-type clusters and linear bis(Tris) ligands. Structural characterization of one of the compounds revealed the formation of a framework structure in the crystal lattice

Communications

through hydrogen bonding interactions between cluster heads and the organic counterions, leading to the formation of approximately 1 nm sized channels in the crystal lattice. Further, the structural analysis of **1** indicates that the size of the void channel in these dimeric hybrids is dependent on the length of the organic linker. In addition, these hybrids are capable of undergoing a remarkable supramolecular self-assembly process in acetone/water mixtures, which leads to the formation of vesicles; the unprecedented formation of such structures from hybrids with large redox-active POM head groups could pave the way for many future materials applications.

Experimental Section

L^1 was prepared according to the published procedure.[24] L^2 (dipentaerythritol) is commercially available. Synthesis of **1**: $TBA_5H_4[P_2V_3W_{15}O_{62}]$[25] (1.0 g, ca. 0.2 mmol) was dissolved in 30 mL of MeCN, then L^1 (0.030 g, 0.1 mmol) was added to the solution. The reaction mixture was refluxed for 6 days in dark. The resulting yellow solution was added drop-wise to excess of diethyl ether with vigorous stirring. The resulting yellow solid was collected and redissolved in minimum volume of MeCN, then reprecipitated by addition to excess diethyl ether. The yellow precipitate thus obtained was isolated by filtration and dried overnight under vacuum; yield 0.90 g (0.09 mmol, 88.39%, based on $TBA_5H_4[P_2V_3W_{15}O_{62}]$). Elemental analysis (%): calcd for $C_{170}H_{376}N_{12}O_{126}P_4W_{30}V_6$ (10 549.55 g mol^{-1}): C 19.35, H 3.59, N 1.59; found: C 18.78, H 3.47, N 1.65. ^{1}H NMR (400 MHz; CD$_3$CN): $\delta = 5.80$ (s, 12 H, -CH$_2$-) and 7.55 (s, 2 H, -NH-) ppm in addition to the TBA resonances. FT-IR (KBr): $\tilde{\nu} = 3444$ (w), 2960 (m), 2933 (m), 2871 (m), 1692 (w), 1484 (m), 1380 (w), 1088 (s), 957 (s), 909 (s), 815 (s), 733 (s), 599 (w), 530 (m), 418 cm^{-1} (w). **2**: The synthetic procedure is same as that for **1** except that L^2 was used instead of L^1; yield 0.85 g (0.08 mmol, 83.8%, based on $TBA_5H_4[P_2V_3W_{15}O_{62}]$). Elemental analysis (%): calcd for $C_{170}H_{378}N_{10}O_{125}P_4W_{30}V_6$ (10 507.56 g mol^{-1}): C 19.43, H 3.63, N 1.33; found: C 20.00, H 3.55, N 1.37. ^{1}H NMR (400 MHz; CD$_3$CN): $\delta = 5.55$ (s, 12 H, -CH$_2$O) and 3.55 (s, 4 H,-CH$_2$-) ppm, in addition to the TBA resonances. FT-IR (KBr): $\tilde{\nu} = 3446$ (w), 2961 (m), 2934 (m), 2872 (m), 1635 (w), 1483 (m), 1379 (w), 1085 (s), 1029 (s), 951 (s), 911 (s), 819 (s), 735 (s), 622 (w), 598 (w), 563 (w), 527 (w), 474 (w), 465 (w), 441 cm^{-1} (w).

[1] a) D.-L. Long, E. Burkholder, L. Cronin, *Chem. Soc. Rev.* **2007**, *36*, 105; b) D.-L. Long, L. Cronin, *Chem. Eur. J.* **2006**, *12*, 3698; c) *Polyoxometalate Chemistry: From Topology via Self-assembly to Applications* (Eds.: M. T. Pope, A. Müller), Kluwer, Dordrecht, **2001**; d) C. L. Hill, *Chem. Rev.* **1998**, *98*, 1.

[2] a) A. Proust, R. Thouvenot, P. Gouzerh, *Chem. Commun.* **2008**, 1837; b) Y.-F. Song, D.-L. Long, L. Cronin, *Angew. Chem.* **2007**, *119*, 3974; *Angew. Chem. Int. Ed.* **2007**, *46*, 3900; c) Y.-F. Song, H. Abbas, C. Ritchie, N. McMillian, D.-L. Long, N. Gadegaard, L. Cronin, *J. Mater. Chem.* **2007**, *17*, 1903; d) Y.-F. Song, N. McMillan, D.-L. Long, J. Thiel, Y. Ding, H. Chen, N. Gadegaard, L. Cronin, *Chem. Eur. J.* **2008**, *14*, 2349.

[3] a) Z. Peng, *Angew. Chem.* **2004**, *116*, 948; *Angew. Chem. Int. Ed.* **2004**, *43*, 930; b) J. L. Stark, A. L. Rheingold, E. A. Maatta, *J. Chem. Soc. Chem. Commun.* **1995**, 1165; c) M. Lu, Y. Wei, B. Xu, C. F.-C. Cheung, Z. Peng, D. R. Powell, *Angew. Chem.* **2002**, *114*, 1636; *Angew. Chem. Int. Ed.* **2002**, *41*, 1566.

[4] a) C. R. Mayer, C. Roch-Marchal, H. Lavanant, R. Thouvenot, N. Sellier, J.-C. Blais, F. Sécheresse, *Chem. Eur. J.* **2004**, *10*, 5517; b) A. Mazeaud, N. Ammari, F. Robert, R. Thouvenot, *Angew. Chem.* **1996**, *108*, 2089; *Angew. Chem. Int. Ed. Engl.* **1996**, *35*, 1961.

[5] a) G. S. Kim, K. S. Hagen, C. L. Hill, *Inorg. Chem.* **1992**, *31*, 5316; b) C. R. Mayer, P. Herson, R. Thouvenot, *Inorg. Chem.* **1999**, *38*, 6152; c) C. R. Mayer, R. Thouvenot, *J. Chem. Soc. Dalton Trans.* **1998**, 7.

[6] C. Boglio, K. Micoine, E. Derat, R. Thouvenot, B. Hasenknopf, S. Thorimbert, E. Lacote, M. Malacria, *J. Am. Chem. Soc.* **2008**, *130*, 4553.

[7] a) M. I. Khan, Q. Chen, D. P. Goshorn, H. Hope, S. Parkin, J. Zubieta, *J. Am. Chem. Soc.* **1992**, *114*, 3341; b) A. Müller, J. Meyer, H. Bögge, A. Stammler, A. Botar, *Chem. Eur. J.* **1998**, *4*, 1388; c) J. W. Han, C. L. Hill, *J. Am. Chem. Soc.* **2007**, *129*, 15094.

[8] a) S. Favette, B. Hasenknopf, J. Vaissermann, P. Gouzerh, C. Roux, *Chem. Commun.* **2003**, 2664; b) Y.-F. Song, N. McMillan, D.-L. Long, S. Kane, J. Malm, M. O. Riehle, C. P. Pradeep, N. Gadegaard, L. Cronin, *J. Am. Chem. Soc.* **2009**, *131*, 1340.

[9] a) Y. Hou, C. L. Hill, *J. Am. Chem. Soc.* **1993**, *115*, 11823; b) H. D. Zeng, G. R. Newkome, C. L. Hill, *Angew. Chem.* **2000**, *112*, 1841; *Angew. Chem. Int. Ed.* **2000**, *39*, 1771; c) C. P. Pradeep, D.-L. Long, G. N. Newton, Y.-F. Song, L. Cronin, *Angew. Chem.* **2008**, *120*, 4460; *Angew. Chem. Int. Ed.* **2008**, *47*, 4388.

[10] J. Li, I. Huth, L.-M. Chamoreau, B. Hasenknopf, E. Lacôte, S. Thorimbert, M. Malacria, *Angew. Chem.* **2009**, *121*, 2069; *Angew. Chem. Int. Ed.* **2009**, *48*, 2035.

[11] a) A. Graff, M. Sauer, P. V. Gelder, W. Meier, *Proc. Natl. Acad. Sci. USA* **2002**, *99*, 5064; b) I. Stanish, D. A. Lowy, C.-W. Hung, A. Singh, *Adv. Mater.* **2005**, *17*, 1194; c) A. V. Kabanov, V. A. Kabanov, *Adv. Drug Delivery Rev.* **1998**, *30*, 49.

[12] C. Ritchie, G. J. T. Cooper, Y.-F. Song, C. Streb, H. Yin, A. D. C. Parenty, D. A. MacLaren, L. Cronin, *Nat. Chem.* **2009**, *1*, 47.

[13] a) S. Zhou, C. Burger, B. Chu, M. Sawamura, N. Nagahama, M. Toganoh, U. E. Hackler, H. Isobe, E. Nakamura, *Science* **2001**, *291*, 1944.

[14] a) T. Liu, E. Diemann, H. Li, A. W. M. Dress, A. Müller, *Nature* **2003**, *426*, 59; b) A. Harada, K. Kataoka, *Science* **1999**, *283*, 65.

[15] J. Zhang, Y.-F. Song, L. Cronin, T. Liu, *J. Am. Chem. Soc.* **2008**, *130*, 14408.

[16] Crystallographic data for $TBA_{10}H_2[(P_2W_{15}V_3O_{59}$-$(OCH_2)_3CNHCO)_2]\cdot 20\,CH_3CN$, **1**·20 CH$_3$CN: $C_{210}H_{436}N_{32}O_{126}P_4W_{30}V_6$, $M_r = 11\,370.93$ g mol^{-1}; block crystal: $0.13 \times 0.11 \times 0.04$ mm^3; $T = 150(2)$ K; monoclinic, space group $C2/c$, $a = 26.8818(4)$, $b = 16.9526(3)$, $c = 69.7195(12)$ Å, $\alpha = 90$, $\beta = 92.592(2)$, $\gamma = 90°$, $V = 31\,739.8(9)$ Å^3, $Z = 4$, $\rho = 2.380$ g cm^{-3}, $\mu(Cu_{K\alpha}) = 21.784$ mm^{-1}, $F(000) = 21\,384$, 35 347 reflections measured, 19 977 unique ($R_{int} = 0.0493$), 1192 refined parameters, $R1 = 0.1267$, $wR2 = 0.2779$ (all data). Crystal data were measured on a Gemini Oxford diffractometer using Cu$_{K\alpha}$ radiation ($\lambda = 1.54184$ Å) at 150(2) K. CCDC 731387 contains the supplementary crystallographic data for this paper. These data can be obtained free of charge from The Cambridge Crystallographic Data Centre via www.ccdc.cam.ac.uk/data_request/cif.

[17] a) H. N. Miras, E. F. Wilson, L. Cronin, *Chem. Commun.* **2009**, 1297; b) D.-L. Long, Y.-F. Song, E. F. Wilson, P. Kögerler, S.-X. Guo, A. M. Bond, J. S. J. Hargreaves, L. Cronin, *Angew. Chem.* **2008**, *120*, 4456; *Angew. Chem. Int. Ed.* **2008**, *47*, 4384.

[18] a) S. W. Provencher, *Biophys. J.*, **1976**, *16*, 29; b) T. Liu, E. Diemann, A. Müller, *J. Chem. Educ.* **2007**, *84*, 526.

[19] C. Schäffer, A. Merca, H. Bögge, A. M. Todea, M. L. Kistler, T. Liu, R. Thouvenot, P. Gouzerh, A. Müller, *Angew. Chem.* **2009**, *121*, 155; *Angew. Chem. Int. Ed.* **2009**, *48*, 149.

[20] A. A. Verhoeff, M. L. Kistler, A. Bhatt, J. Pigga, J. Groenewold, M. Klokkenburg, S. Veen, S. Roy, T. Liu, W. K. Kegel, *Phys. Rev. Lett.* **2007**, *99*, 066104.

[21] M. L. Kistler, A. Bhatt, G. Liu, D. Casa, T. Liu, *J. Am. Chem. Soc.* **2007**, *129*, 6453.

[22] S. Kim, Y. Kim, J. Lee, W. Shin, M. Lee, S.-J. Kim, *Inorg. Chim. Acta* **2007**, *360*, 1890.

[23] P. P. Mishra, J. Jing, L. C. Francesconi, T. Liu, *Langmuir* **2008**, *24*, 9308.

[24] G. E. DuBois, B. Zhi, G. M. Roy, S. Y. Stevens, M. Yalpani, *J. Chem. Soc. Chem. Commun.* **1992**, 1604.

[25] R. G. Finke, B. Rapko, R. J. Saxton, P. J. Domaille, *J. Am. Chem. Soc.* **1986**, *108*, 2947.